ACCOUNTS
of chemical research

The Heterogeneous Nature of Cu^{2+} Interactions with Alzheimer's Amyloid-β Peptide

SIMON C. DREW*,† AND KEVIN J. BARNHAM‡

†*Max Planck Institute for Bioinorganic Chemistry, 45470 Mülheim an der Ruhr, Germany, and* ‡*Department of Pathology, The Bio21 Molecular Science and Biotechnology Institute, and the Mental Health Research Institute, The University of Melbourne, Victoria 3010, Australia*

RECEIVED ON JANUARY 25, 2011

CONSPECTUS

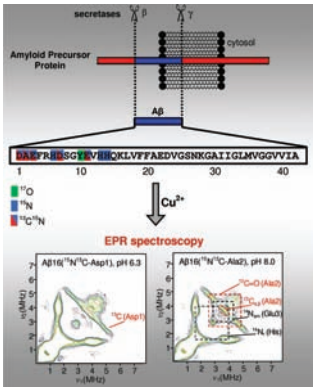

Alzheimer's disease (AD) is a neurodegenerative disorder characterized by progressive cognitive and memory impairment. Within the brain, senile plaques, which comprise extracellular deposits of the amyloid-β peptide (Aβ), are the most common pathological feature of AD. A high concentration of Cu^{2+} is found within these plaques, which are also areas under oxidative stress. Laboratory work has shown that in vitro Aβ will react with Cu^{2+} to induce peptide aggregation and the production of reactive oxygen species. As such, this interaction offers a possible explanation for two of the defining pathological features observed in the AD brain: the presence of amyloid plaques, which consist largely of insoluble Aβ aggregates, and the abundant oxidative stress therein. Researchers have accordingly put forth the "metals hypothesis" of AD, which postulates that compounds designed to inhibit Cu^{2+}/Aβ interactions and redistribute Cu^{2+} may offer therapeutic potential for treating AD.

Characterization of the pH-dependent Cu^{2+} coordination of Aβ is fundamental to understanding the neurological relevance of Cu^{2+}/Aβ interactions and aiding the design of new therapeutic agents. In an effort to shed light on the problem, many experimental and theoretical techniques, using a variety of model systems, have been undertaken. The preceding decade has seen numerous conflicting spectroscopic reports concerning the nature of the Cu^{2+}/Aβ coordination. As the number of studies has grown, the nature of the pH-dependent ligand environment surrounding the Cu^{2+} cation has remained a point of contention. In large part, the difficulties can be attributed to inappropriate choices of the model system or to methods that are incapable of quantitatively delineating the presence and identity of multiple Cu^{2+} coordination modes.

Electron paramagnetic resonance (EPR) is the method of choice for studying paramagnetic metal−protein interactions. With the introduction of site-specific ^{15}N, ^{17}O, and ^{13}C isotopic labels and the application of advanced techniques, EPR is capable of eliminating much of the ambiguity. Recent EPR studies have produced the most definitive picture of the pH-dependent Cu^{2+} coordination modes of Aβ and enabled researchers to address the inconsistencies present in the literature.

In this Account, we begin by briefly introducing the evidence for a role of Cu^{2+} in AD as well as the potential physiological and therapeutic implications of that role. We then outline the EPR methodology used to resolve the molecular details of the Cu^{2+}/Aβ interactions. No drugs are currently available for altering the course of AD, and existing therapies only offer short-term symptomatic relief. This focused picture of the role of Cu^{2+} in AD-related plaques offers welcome potential for the development of new methods to combat this devastating disease.

1. Cu/Aβ interactions in Alzheimer's Disease

Alzheimer's disease (AD) is the most common age related neurodegenerative disease. Currently, there are no disease modifying drugs and existing therapies only offer short-term symptomatic relief. Two of the defining pathological indicators of AD are the presence of extracellular amyloid deposits, consisting primarily of the β-amyloid (Aβ) peptide, and oxidative stress.[1] The 39−43 amino acid Aβ peptide is cleaved from the transmembrane amyloid precursor protein (APP) by β and γ sectretases (Figure 1A,B). While APP possesses physiological functions, most recently being proposed to play the role of a ferroxidase in the central nervous system,[2] Aβ forms neurotoxic oligomers that are likely to be responsible for the synaptic dysfunction in AD.[3] In this

Published on the Web 06/29/2011 www.pubs.acs.org/accounts
10.1021/ar200014u © 2011 American Chemical Society

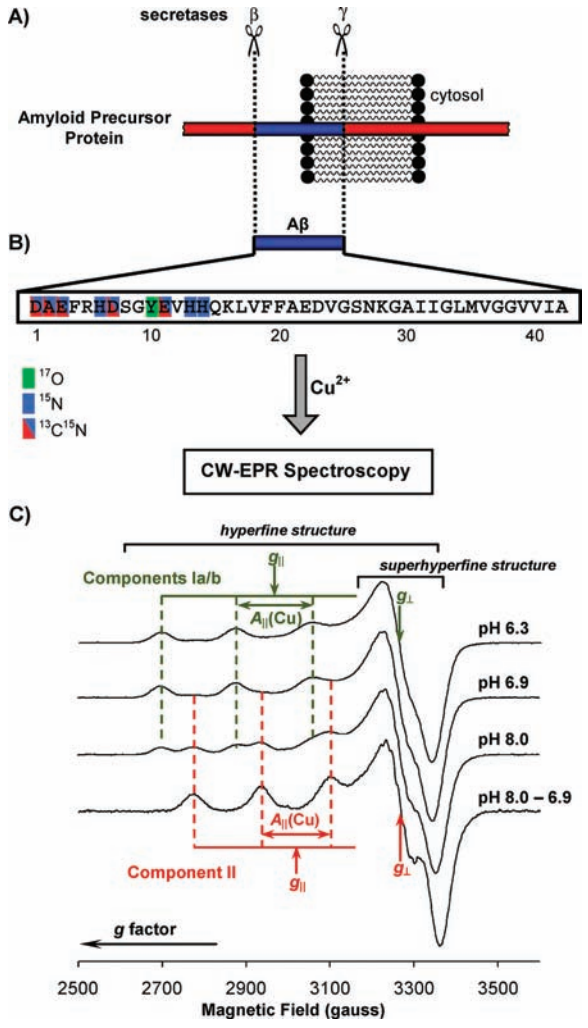

FIGURE 1. (A) Processing of the amyloid precursor protein (APP) via the amyloidogenic pathway to generate the toxic Aβ peptide; heterogeneous γ secretase cleavage generates peptides of length 39−43 a.a. (B) Amino acid sequence of Aβ1−42 (Aβ42). Synthetic peptides can be generated with isotopic labels placed on individual atoms of specific residues for CW- and pulsed-EPR studies. (C) X-band CW-EPR spectra of Aβ16 (unlabeled) with 0.9 equiv $^{65}Cu^{2+}$ in PBS at 77 K, showing the pH dependence of the physiologically relevant Cu^{2+} coordination modes. Hyperfine structure is seen due to interaction of the metal-centered unpaired electron with the magnetic moment of the ^{65}Cu nucleus (the fourth $A_{||}$(Cu) hyperfine line is hidden under the $g_{\perp}$ features). First approximations to the principal g and A values can be obtained directly from the spectrum as indicated. Superhyperfine (shf) structure is also resolved due to interactions of the unpaired electron with ligand nuclei and the Cu nucleus ($A_{\perp}$(Cu)). By varying the isotopic content of the ligand nuclei, changes in the shf structure can be observed. The resolution of shf structure is aided using monoisotopic Cu^{2+} and lower spectrometer operating frequencies (e.g., S-band).[21,24,26,28]

regard, the defining features of Aβ aggregation, oxidative stress, and neuronal cell death in AD may be explained by the interactions of Aβ with Cu^{2+}. Synthetic Aβ reacts with Cu^{2+} to form aggregates and generate reactive oxygen species by reducing coordinated Cu^{2+} to Cu^{+} with the concomitant oxidation of other moieties such as thiols, ascorbate, lipids, or Aβ side chains.[4−6] Divalent copper also potentiates the toxicity of Aβ to neuronal cell cultures,[7] which may be related to soluble oligomeric species generated by oxidation and covalent cross-linking of Aβ side chains.[4,5] Disease-modifying strategies based upon the rational design of therapeutics that inhibit the formation of toxic Aβ species as well as restoring metal homeostasis would be facilitated by detailed knowledge of the Cu^{2+}/Aβ interface.[8] However, until recently, limited consensus on any of the Cu^{2+}/Aβ coordination modes could be obtained.

2. Defining the Cu^{2+}/Aβ Coordination Sphere: The Problems

Similar to other metalloproteins, more than one Cu^{2+} coordination mode is accessible to Aβ at physiological pH. This was clear from the pH-dependent equilibrium between two distinct species, commonly designated as "component I" and "component II", that could be identified by continuous-wave electron paramagnetic resonance (CW-EPR) spectra of a variety of Cu^{2+}/Aβ complexes (Figure 1C).[9−15] Paramagnetic NMR implicated the participation of all three His residues of Aβ in high-affinity Cu^{2+} coordination,[9,14,16] but the manner in which they coordinated together with the potential involvement of the amino terminus (NH_2),[10−14] the side chain carboxylate oxygen (COO^-) of Asp1, Glu3, Asp7, and Glu11,[9,10,14,17] the phenolic oxygen of Tyr10,[18] and a backbone carbonyl oxygen (C=O)[10] remained unresolved. Proposed equatorial ligand spheres for component I included $\{NH_2^{D1}, N_{Im}^{H6}, N_{Im}^{H13}, N_{Im}^{H14}\}$,[12] $\{COO^{-\,D1}, N_{Im}^{H6}, N_{Im}^{H13}, N_{Im}^{H14}\}$,[14] $\{NH_2^{D1}, O, N_{Im}^{H6}, N_{Im}^{H13}\}$,[13] and $\{NH_2^{D1}, COO^-, N_{Im}^{H13}, N_{Im}^{H14}\}$.[10] For component II, $\{NH_2^{D1}, N_{Im}^{H6}, N_{Im}^{H13}, N_{Im}^{H14}\}$[14] and $\{NH_2^{D1}, N^-, C{=}O, N_{Im}^{H6}\}$[10] ligand spheres had been proposed, while in other cases participation of deprotonated backbone amide nitrogen (N_{am}) ligands was only inferred.[12] In some instances, coordination near pH 7.4 was examined without accounting for the presence of more than one coordination mode, including EXAFS,[17] paramagnetic NMR,[16] and electron spin echo envelope modulation (ESEEM) studies.[19]

In addition to being able to delineate different coordination modes, the EPR spectroscopic parameters $g_{||}$ and $A_{||}$(Cu) (Figure 1C) have commonly been used to infer the number of nitrogen and oxygen ligands in Cu^{2+}/Aβ complexes,[10,12−14] although the relationship is at best qualitative in practice.[20,21] Combining such information with complementary methods such as UV−vis and circular dichroism provides

additional information about the type of ligands involved by identifying d−d and ligand-to-metal charge transfer transitions, but assigning such transitions to a specific coordination mode when many modes overlap remains difficult.

To identify the residues involved, point mutations or chemical modifications have frequently been introduced,[10,12,13,15,22] with the aim of attributing any spectral changes to a direct role of the modified residue in Cu^{2+} coordination. However, mutating or blocking a coordinating residue of the native complex will cause a major rearrangement of the first coordination sphere to replace the lost ligand while counterintuitively resulting in only minor spectral changes if the blocked or mutated ligand is replaced by another of the same type.[12,22] Mutations and other modifications may also alter the coordination environment without the affected residue being directly coordinated to the metal ion.

3. Defining the Cu^{2+}/Aβ Coordination Sphere: The Solution

A superior method for studying Cu^{2+} coordination of Aβ is to introduce *site-specific isotopic labels* to the surrounding nuclei and examine the resulting spectral changes using EPR methods, which directly probe the electron−nuclear interactions. The theory and applications of EPR, in particular CW-EPR, ESEEM, and electron−nuclear double resonance (ENDOR) are described in comprehensive texts,[21,23] and the EPR of Cu^{2+} complexes and proteins has also been reviewed.[24,25] Using CW-EPR, the goal is to resolve and observe changes in the metal−ligand superhyperfine (shf) pattern (Figure 1C) that accompany a change in both the nuclear spin I and magnetic moment g_n upon varying the isotopic content of a specific nucleus. Much the same way one aims to infer the coordination of specific residues by observing spectral changes (e.g., in $g_{\|}$ and $A_{\|}$(Cu)) upon introducing a point mutation, this can be more definitively achieved by observing spectral changes (e.g., in the shf structure of CW-EPR spectra, or in the nuclear frequencies in ESEEM and ENDOR spectra) following introduction of a site specific isotopic label. The isotopic labeling approach is more sensitive to pH dependent changes in ligand environment and does not perturb the native structure of the metal−protein complex. Its utility has been demonstrated in the study of the Cu^{2+} coordination environment of the prion protein (PrP) octarepeat fragment, with its accuracy in this instance being verified by X-ray crystallography.[26] Reference 26 affords an excellent review of the application of EPR and isotopic labeling to the structure and function of Cu^{2+} coordination to PrP and provides much of the framework for our studies of Aβ.

Although pulsed EPR methods offer greater resolution, CW-EPR can be advantageous when many coordination modes overlap because the density of shf lines in each mode is multiplicative with respect to the number of interacting nuclei (following a $\Pi_i(2I_i + 1)$ rule, where I_i is the nuclear spin of the ith nucleus[27]); hence, changing the isotopic content of a single ligand alters the entire shf spectrum. This compares with ENDOR spectroscopy, for example, which is also sensitive to directly coordinated ligands, where the density of nuclear hyperfine lines is additive with respect to the number of interacting nuclei (producing $\Sigma_i(4I_i)$ lines[27]); here, altering the isotopic content of a single ligand affects only $4I$ hyperfine lines and not the entire spectrum, making it more difficult to assign the ligand to a specific coordination mode when many modes are copopulated. This limitation also applies to some degree to ESEEM spectroscopy, although combination frequencies of hyperfine lines corresponding to ligands participating in the same coordination mode can provide additional information.

4. Nitrogen Coordination of Cu^{2+}/Aβ at Low pH

Between pH 6 and 7, the CW-EPR spectrum is dominated by component I (Figure 1C).[6,12−15] Figure 2A shows the effects of introducing ^{15}N labels at residues Asp1, His6, His13, and His14 on the CW-EPR spectrum of Cu^{2+}/Aβ16 at pH 6.3. A perturbation of the shf pattern was immediately obvious when each of the above residues was (uniformly) ^{15}N-labeled, which suggests, assuming a single coordination mode, that the equatorial coordination at low pH comprises a 4N coordination sphere involving a nitrogen ligand from the amino terminus and one from each histidine. However, numerical simulations of the unlabeled Cu^{2+}/Aβ complex supported a $\{O, {}^{14}N, {}^{14}N, {}^{14}N\}$ coordination sphere, suggesting the above interpretation was simplistic.[28] A full understanding of the Cu^{2+} coordination at pH < 7 therefore required a re-evaluation of the assumption that the component I signal represented a single species. The solution of the problem involved invoking the presence of a second coordination mode with principal g and $A(^{65}Cu)$ parameters indistinguishable from component I at S-band and X-band microwave frequencies; these two coordination modes were termed components Ia and Ib.[28] In keeping with this, potentiometric and spectroscopic studies of Cu^{2+}/Aβ16 suggested two $\{NH_2, O, N_{Im}, N_{Im}\}$ coordination modes with identical principal $g_{\|}$ and $A_{\|}(^{63,65}Cu)$ parameters were approximately equally populated and accounted for ca. 95%

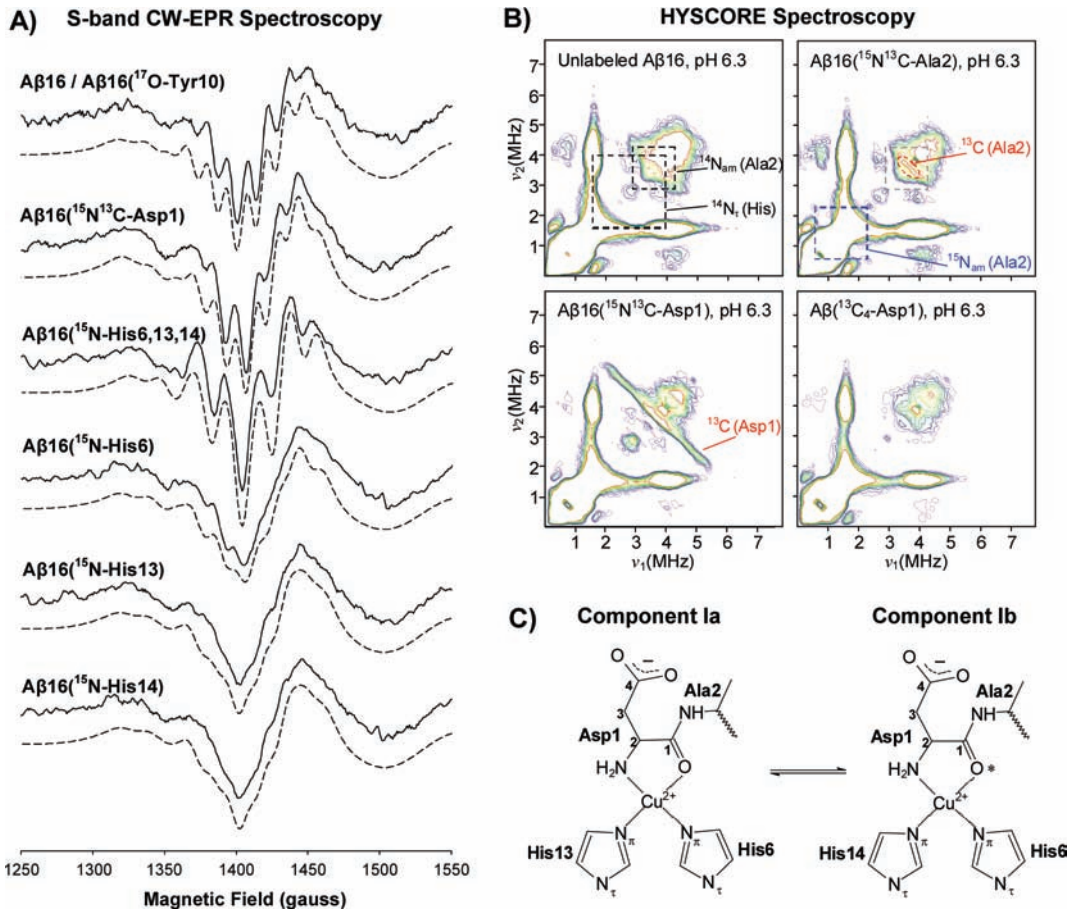

FIGURE 2. (A) Comparison of experimental (full lines) and simulated (dashed lines) second derivative S-band CW-EPR spectra of $^{65}Cu^{2+}$/Aβ16 and isotopically labeled analogues at pH 6.3 (expanded about the $g_\perp$ region), showing the changes in shf structure accompanying site-specific ^{15}N labeling of Asp1, His6, His13, and His14, due to the rescaling of the ^{14}N shf interactions by $g_n(^{15}N)/g_n(^{14}N) = 1.40$. Labeling of the phenolic oxygen of Tyr10 with ^{17}O (30%) had no effect on the shf structure.[28] Simulations were based upon a summation of components Ia and Ib shown in panel C. (B) X-band HYSCORE spectra of $^{65}Cu^{2+}$/Aβ16 and isotopically labeled analogues obtained near $g_\perp$ at pH 6.3. Carbon-13 labeling of Asp1 revealed correlation ridges dominated by the α-carbon ($^{13}C_2$) due to coordination of NH_2^{D1} and by the ε-carbon ($^{13}C_1$) due to coordination of $C{=}O^{D1}$, while the absence of these ridges upon selective labeling of the carboxylate ($^{13}C_4$) ruled out side chain carboxylate coordination. Cross-peaks corresponding to double quantum transitions from a noncoordinating $^{14}N_{am}$ appear in the HYSCORE spectrum of Cu^{2+}/Aβ16 are replaced by $^{15}N_{am}$ cross-peaks in the spectrum of Cu^{2+}/Aβ16($^{15}N^{13}C$-Ala2), implicating $C{=}O^{D1}$ coordination. The low intensity of these features suggests that $C{=}O^{D1}$ might coordinate in only one of the two modes, which is indicated by the asterisk (*) in panel (C). (C) Schematic of the coordination spheres of components Ia and Ib, as deduced from the data in panels (A) and (B). (Figure adapted with permission from refs 28 and 31. Copyright 2009 American Chemical Society.)

of the Cu^{2+} species in solution at pH 6.3;[10] however, it was not possible to unambiguously assign the residues involved. By using site-specific isotopic labeling and careful simulations of the shf structure, it could be shown that both modes involve equatorial nitrogen coordination of the amino terminus and His6, while the third nitrogen ligand is supplied by His13 in component Ia and His14 in component Ib.[28] ENDOR spectroscopy of Cu^{2+}/Aβ16(^{15}N-Asp1) also later confirmed the participation of NH_2^{D1}.[37] Figure 2A displays the simulations of the shf structure obtained from a weighted summation of $\{NH_2^{D1}, O, N^{H6}, N^{H13}\}$ and $\{NH_2^{D1}, O, N^{H6}, N^{H14}\}$ modes, which are an excellent reproduction of the observed experimental spectra. Although the strong similarity of the shf patterns of Cu^{2+}/Aβ16(^{15}N-His13) and Cu^{2+}/Aβ16(^{15}N-His14) provided a clue to the above interpretation, the full complement of ^{15}N-labeled peptides, including the triple labeled Aβ16(^{15}N-His6,13,14), were required to unambiguously determine the identity of the coordinating ligands in each component. Since the His residues were uniformly ^{15}N-labeled, CW-EPR could not distinguish between His coordination via the backbone amide or the side chain imidazole nitrogen (N_{Im}). However, HYSCORE spectroscopy of Cu^{2+}/Aβ16(^{15}N-His6), Cu^{2+}/Aβ16(^{15}N-His13), and Cu^{2+}/Aβ16(^{15}N-His14) confirmed the coordination via N_{Im} through the appearance of ^{15}N cross-peaks from the distal nitrogen in each instance.[28]

An equilibrium between $\{NH_2^{D1}, O, N_{Im}^{H6}, N_{Im}^{H13}\}$ and $\{NH_2^{D1}, O, N_{Im}^{H6}, N_{Im}^{H14}\}$ modes was qualitatively consistent with the greater intensity of the ^{15}N cross-peaks observed in the HYSCORE spectrum of Cu^{2+}/Aβ16(^{15}N-His6) as compared with Cu^{2+}/Aβ16(^{15}N-His13) and Cu^{2+}/Aβ16(^{15}N-His14).[28] However, caution should be excerised when interpreting the relative peak amplitudes in randomly oriented HYSCORE spectra of multinuclear systems[29] (and additional intensity of ^{15}N cross peaks in the HYSCORE spectrum of Cu^{2+}/Aβ16(^{15}N-His6) could in principle also result from carbonyl coordination of Arg5; see sections 5, 7, and 8). It is the multiplicative dependence of the CW-EPR spectrum on the ligand shf interactions[27] that both predicted the presence of components Ia and Ib and provided the definitive nitrogen ligand assignment in each.

5. Oxygen Coordination of Cu^{2+}/Aβ at Low pH

Early studies proposed the phenolic oxygen of Tyr10 as a possible O ligand,[9,18] although no absorption near 400 nm to suggest a $O^-_{Tyr} \rightarrow Cu^{2+}$ charge-transfer band was observed.[10] Moreover, compared with the unlabeled Cu^{2+}/Aβ16 complex, no perturbation of the shf structure was observed between pH 6.3 and 8.0 when the phenolic oxygen of Tyr10 was ^{17}O-labeled, ruling out Tyr10 coordination.[28] Although it is more difficult to unambiguously assign the nuclear frequencies in HYSCORE spectra to individual coordination modes (section 3), HYSCORE spectroscopy in conjunction with ^{13}C-labeling of the next-nearest nuclei provides a valuable alternative when ^{17}O labeling is either unfeasible or prohibitively expensive. Until very recently, the oxygen ligand in component I (a and b) was believed to be a carboxylate,[6,10,14,30] most probably that of Asp1.[6,30] Indeed, HYSCORE studies of Cu^{2+}/Aβ16($^{13}C^{15}$N-Asp1) (with uniform ^{13}C labeling) revealed ^{13}C correlation ridges at pH 6.3 not inconsistent with the presence of the carboxylate (the $^{13}C_4$ nucleus in Figure 2C) and two bonds from Cu^{2+} (Figure 2B).[28] However, since CW-EPR already showed that NH_2^{D1} coordinates in components Ia and Ib (section 4), the α-carbon ($^{13}C_2$), likewise being two bonds from Cu^{2+}, should also contribute ^{13}C spectral features when Asp1 is uniformly ^{13}C-labeled.[28] To resolve this uncertainty, a specific $^{13}C_4$ label was introduced on the carboxylate of Asp1, whereupon the correlation ridges disappeared (Figure 2B), definitively ruling out equatorial coordination of the carboxylate of Asp1.[31] The only observable ^{13}C feature in this instance was a diagonal peak at the ^{13}C Larmor frequency ($a_{iso}(^{13}C)| < 1$ MHz) when the HYSCORE spectrum was acquired at a magnetic field near $g_{||}$, present at both pH 6.3 and pH 8.0, indicating at most axial coordination of the Asp1 carboxylate or noncoordination.[31,32] Interestingly, the carboxylate side chain *does* coordinate equatorially when Aβ is isomerized at Asp1, as demonstrated by the appearance of ^{13}C cross-peaks in the HYSCORE spectra of Cu^{2+}/Aβ16($^{13}C_4$-isoAsp1).[33] Isomerization of Asp1 results in a dominant $\{NH_2^{D1}, COO^{-D1}, 2N_{Im}\}$ mode between pH 6 and 8 via the formation of a highly stable five-membered chelate ring.[33] Although Aβ42(isoAsp1) is found in AD plaques,[34] the physiological significance of the different Cu^{2+} coordination associated with this post-translational modification remains to be established.

Similar to the case of Cu^{2+}/Aβ16(isoAsp1), evidence for the formation of a five-membered chelate ring at the N-terminus was also found for Cu^{2+}/Aβ16 at pH 6.3 in the form of weak cross-peaks near (3, 4) MHz in the HYSCORE spectrum (Figure 2B), consistent with so-called double quantum transitions of a noncoordinating $^{14}N_{am}$.[25,26,28,31] When an Aβ16-($^{15}N^{13}$C-Ala2) analogue was studied under the same conditions, these $^{14}N_{am}$ cross-peaks were replaced with peaks centered upon the ^{15}N Larmor frequency (near 1.45 MHz in Figure 2B).[31] The presence of the weakly coupled ($|a_{iso}(^{13}C)| < 1$ MHz) α-carbon of Ala2 four bonds from Cu^{2+}, also manifested in Cu^{2+}/Aβ16($^{15}N^{13}$C-Ala2) as features close to the diagonal near the Larmor frequency of ^{13}C (near 3.6 MHz in Figure 2B). Together, these observations demonstrated that N_{am}^{A2} is three bonds from Cu^{2+}, thereby implicating coordination of $C{=}O^{D1}$ in component I (Figure 2C).[31] This was an unexpected assignment given the available experimental evidence at that time.[6,30] Interestingly, similar results have been obtained for an Aβ16 peptide containing the familial A2V mutation, where the first coordination sphere of each mode appears unchanged except for a modest shift in the pH dependence due to changes in the outer coordination sphere.[33]

Although the relative peak amplitudes in HYSCORE spectra of multinuclear systems should be interpreted with caution,[29] the weakness of the N_{am}^{A2} cross-peaks suggested that $C{=}O^{D1}$ may not be an oxygen ligand common to both components Ia and Ib.[31] To investigate the possibility that other acidic side chains coordinate in either components Ia or Ib, site-specific ^{13}C labels were also introduced on Glu3, Asp7 and Glu11. In no case was a characteristic set of ^{13}C cross-peaks observed (at pH 6.3 or 8.0) to support Glu3, Asp7, or Glu11 as carboxylate ligands.[31] Moreover, by analogy with the experimental features that result from $C{=}O^{D1}$ coordination at low pH, no appearance of ^{15}N

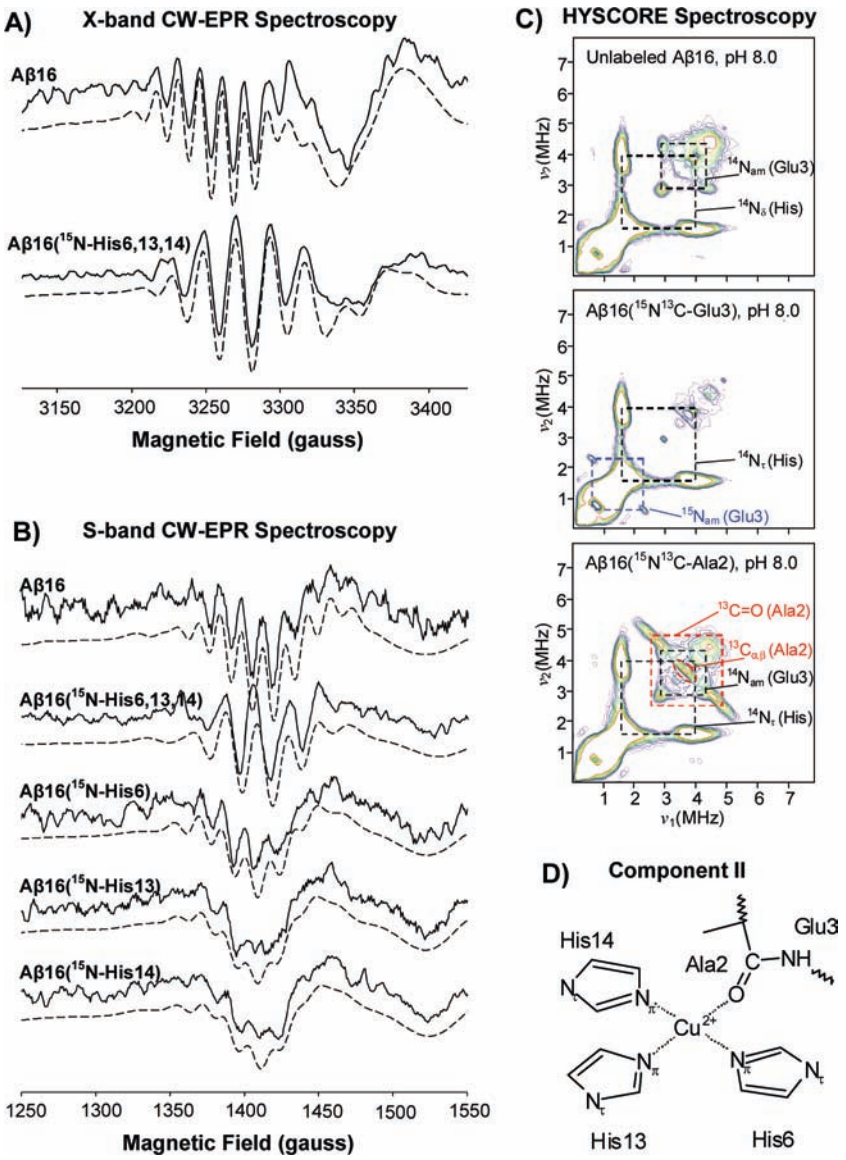

FIGURE 3. Comparison of experimental (full lines) and simulated (dashed lines) second derivative (A) X-band and (B) S-band CW-EPR spectra of component II (expanded about the $g_\perp$ region), isolated as described in section 3, showing changes in shf structure accompanying site-specific ^{15}N labeling of His6, His13 and His14. (C) X-band HYSCORE spectra of Cu^{2+}/Aβ16 and isotopically labeled analogues obtained near $g_\perp$ at pH 8.0. The $^{15}N_{am}$ cross-peaks in the spectrum of Cu^{2+}/Aβ16($^{15}N^{13}C$-Glu3) and the strong ^{13}C correlation ridges in the spectrum of Cu^{2+}/Aβ16($^{15}N^{13}C$-Glu3) provide definitive evidence of $C{=}O^{A2}$ coordination. (D) The component II coordination sphere proposed from the data in panels (A)–(C). The coordination sphere is drawn schematically only and possesses tetrahedral distortion.[33] HYSCORE spectroscopy of Cu^{2+}/Aβ16($^{13}C_4$–Asp1) (not shown) provided conditional evidence[32] for axial coordination of the carboxylate group of Asp1 (not drawn).[31] (Figure adapted with permission from refs 28 and 31. Copyright 2009 American Chemical Society.)

cross-peaks or concomitant disappearance of $^{14}N_{am}$ features near (3, 4) MHz was observed following ^{15}N-labeling of Glu3, Asp7, or Glu11 to support Ala2, His6, or Tyr10, respectively, as equatorial C=O ligands in components Ia/b.[31] Alternative equatorial C=O ligands have more recently been proposed, in particular bidentate coordination of the carbonyl and side chain of His6, His13, or His14.[35] However, $C{=}O^{H6}$ coordination appears unlikely in light of the above findings.

6. Nitrogen Coordination of Cu^{2+}/Aβ at High pH

Of the additional modes populated above pH 7, only component II is likely to be significantly populated near pH 7.4.[10] Quantitative assessment of its coordination sphere is nevertheless complicated by the equilibrium with higher pH coordination modes in addition to components Ia/b at lower pH. In particular, beyond pH 8 contributions from higher pH coordination modes become significant.[10,33] Using CW-EPR, however, component II can be satisfactorily isolated by

spectral algebra as depicted in Figure 1C. Numerical simulations of the component II shf spectrum of Cu^{2+}/Aβ16 indicated a {O, ^{14}N, ^{14}N, ^{14}N} coordination sphere (Figure 3A).[28] Compared with the unlabeled peptide, a major perturbation of the shf pattern resulted when all three His residues were uniformly ^{15}N-labeled and the shf spectrum of Cu^{2+}/Aβ16(^{15}N-His6,13,14) could be simulated with a {O, ^{15}N, ^{15}N, ^{15}N} ligand sphere (Figure 3A).[28] To identify the specific His residues involved, His6, His13, and His14 were also individually ^{15}N-labeled and the shf structure was examined using *S*-band CW-EPR. The component II shf patterns from Cu^{2+}/Aβ16(^{15}N-His6), Cu^{2+}/Aβ16(^{15}N-His13), and Cu^{2+}/Aβ16(^{15}N-His14) all differed from that of the unlabeled peptide (Figure 3B), while the component II shf spectra of Cu^{2+}/Aβ16(^{15}N^{13}C-Asp1) and Cu^{2+}/Aβ16 appeared comparable.[28] Numerical simulations employing a {O, ^{15}N, ^{14}N, ^{14}N} coordination sphere for Cu^{2+}/Aβ16(^{15}N-His6), and similarly for Cu^{2+}/Aβ16(^{15}N-His13) and Cu^{2+}/Aβ16(^{15}N-His14), further supported the assignment of a {O, N_{Im}^{H6}, N_{Im}^{H13}, N_{Im}^{H14}} coordination mode (Figure 3B).

HYSCORE spectroscopy of Cu^{2+}/Aβ16(^{15}N^{13}C-Asp1) at pH 8.0 suggested a diminished ^{13}C cross peak intensity relative to the signal observed at pH 6.3, while HYSCORE spectroscopy of Cu^{2+}/Aβ16(^{15}N-His6), Cu^{2+}/Aβ16(^{15}N-His13), and Cu^{2+}/Aβ16(^{15}N-His14) at pH 8.0 provided conditional evidence for the side chain coordination of all three His residues in component II.[28] Weak combination peaks corresponding to multiples of the His $^{14}N_{\tau}$ frequencies that are often observed for multihistidine Cu^{2+} coordination[25] are not clearly identifiable at high pH (Figure 3C);[28,31,37] however, their absence is not clear-cut evidence against such coordination[36] and N_{am}^{E3} cross peaks (see section 7) may mask or suppress weak combination peaks. Indeed, the intensity of the combination peaks in HYSCORE spectra Cu^{2+}/Aβ16 and Cu^{2+}/Aβ16(isoAsp1) peptides at pH 6.9 are dramatically different, yet both coordinate via two His.[33] The $g_{\|}/A_{\|}$(^{63}Cu) ratio for component II falls outside the normal range for square planar Cu^{2+} complexes, suggesting a shift to a more distorted geometry,[33] which is conceivably required to accommodate simultaneous coordination of all three His residues. While the signal-to-noise ratio following spectral subtraction was lower, the simulations in Figure 3A,B provide reasonable fits that appear self-consistent across four labeled peptide analogues and two microwave frequencies.[28]

Following the original proposal of {NH_2, CO, N_{am}, N_{Im}} coordination from potentiometric studies,[9] an alternative {NH_2^{D1}, O N_{am}^{A2}, $N_{Im}^{H6/H13/H14}$} mode of nitrogen coordination has more recently been proposed for component II using the isotopic labeling approach, where all His residues are assumed exchangeable.[35,37] In particular, HYSCORE spectra of Cu^{2+}/Aβ16(^{13}C-Asp1) and ENDOR spectra of Cu^{2+}/Aβ16(^{15}N-Ala2) provided clear evidence of coordination of $NH_2^{D1}$and N_{am}^{A2} at pH 9.0, where components Ia and Ib were no longer visibly populated.[37] However, even at maximum occupancy, component II is predicted to account for only 60% of Cu^{2+} speciation, with at least 20% being a 4N coordination mode postulated to be {NH_2, $2N^-$, N_{Im}}.[10] The shf structure from CW-EPR of Cu^{2+}/Aβ16(^{15}N-Ala2) also supported N_{am}^{A2} coordination at pH 11,[37] but 4N coordination distinct from component II occurs at this pH.[10,33] Conversely, difference spectra (pH 8.0 − pH 6.9) showed a negligible shift in the positions of the component II shf lines of Cu^{2+}/Aβ16(^{15}N^{13}C-Ala2) as compared with Cu^{2+}/Aβ16,[33] whereas ^{15}N-labeling of a single nitrogen ligand should have a more marked effect.[28]

The proposition of His6, His13, and His14 as "equivalent ligands" in exchange in a {NH_2^{D1}, O, N_{am}^{A2}, $N_{Im}^{H6/H13/H14}$} model of component II[35,37] would (assuming no Cu^{2+} bridging of Aβ monomers) require a superposition of {NH_2^{D1}, O, N_{am}^{A2}, N_{Im}^{H6}}, {NH_2^{D1}, O, N_{am}^{A2}, N_{Im}^{H13}}, and {NH_2^{D1}, O, N_{am}^{A2}, N_{Im}^{H14}} coordination modes with highly similar principle $g_{\|}$ and $A_{\|}$(Cu) parameters (despite the reorganization of the peptide backbone). The distinction between a superposition of these three modes and a {O, N_{Im}^{H6}, N_{Im}^{H13}, N_{Im}^{H14}} mode should be apparent in the shf pattern. In the former case, the spectrum of Cu^{2+}/Aβ16(^{15}N-His6,13,14) should be a superposition of three modes with similar 2 × ^{14}N/1 × ^{15}N type coordination, since in each only a single His residue would be ^{15}N-labeled. Yet the component II shf spectrum of Cu^{2+}/Aβ16(^{15}N-His6,13,14) appears to be 3 × ^{15}N, both by simulations (Figure 3A) and by comparison with (uniformly) ^{15}N-labeled Aβ40.[28] Certainly, it will be interesting to re-evaluate the multifrequency component II shf spectra of Cu^{2+}/Aβ16(^{15}N-Asp1), Cu^{2+}/Aβ16(^{15}N^{13}C-Ala2), and Cu^{2+}/Aβ16(^{15}N-His6,13,14) in the context of a {NH_2, O, N_{am}, N_{Im}} model of component II.

7. Oxygen Coordination of Cu^{2+}/Aβ at High pH

A clue to the identity of the equatorial oxygen ligand in component II was first obtained from HYSCORE spectroscopy of Cu^{2+}/Aβ at pH 8.0, which revealed cross-peaks near (3, 4) MHz characteristic of the presence of a noncoordinating $^{14}N_{am}$.[28] By analogy with the case described at low pH (section 5), this implied the coordination of a carbonyl oxygen. Although previously proposed,[10] no direct evidence

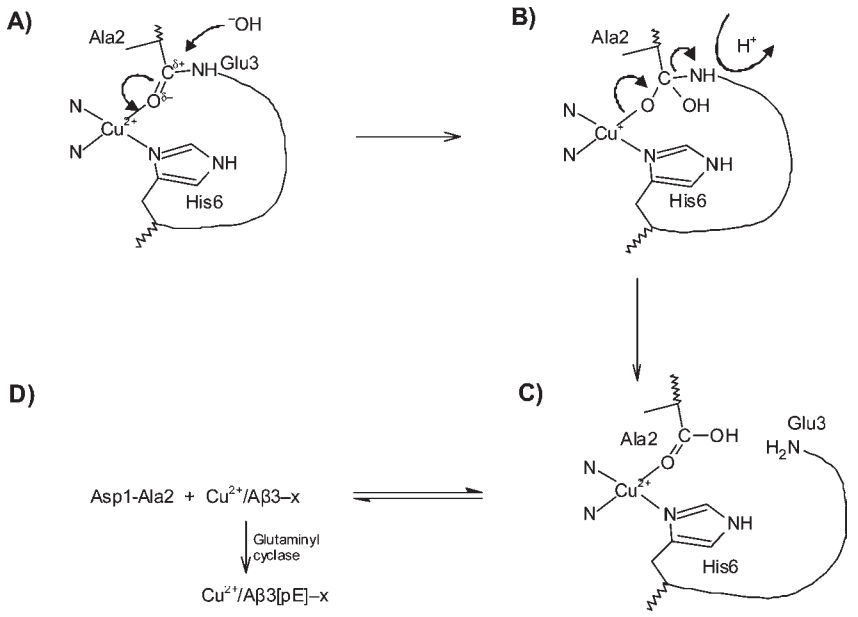

FIGURE 4. Possible mechanism of amide hydrolysis leading to Aβ3$-x$ (x = 40, 42) species. (a) Coordination of Ala2 via component II polarizes the carbonyl carbon, allowing nucleophilic attack by OH^- (or other biological nucleophiles, such as thiols, ascorbate or amino acid side chains), leading to (b) formation of a tetrahedral intermediate (TI), via a Cu^+ oxidation state (shown) or alternatively via $Cu^{2+}-O^-$−C−; (c) subsequent breakdown of the TI involving cleavage of the amide bond and protonation of the leaving amide (possibly by a nearby amino acid side chain); (d) Cu^{2+} coordination of truncated Aβ3$-x$ and formation of Aβ3[pE]$-x$, both spontaneously and by glutaminyl cyclase. Transient interactions with other cofactors in vivo could be required to promote formation and breakdown of the TI. The geometry of the coordinating ligands is drawn schematically only. (Figure adapted from Drew et al.[33])

for this existed and it generally remained a disregarded ligand assignment.[30] Nevertheless, isotopic labeling and HYSCORE spectroscopy definitively confirmed the carbonyl coordination of Ala2 by revealing a shift in the $^{14}N_{am}$ cross peaks upon ^{15}N-labeling of Glu3 and the appearance of ^{13}C correlation ridges upon ^{13}C-labeling of Ala2 (Figure 3C).[31] Isotopic labeling also showed that this carbonyl coordination persists even for the A2V familial mutant.[33] Further to this, HYSCORE spectroscopy of Cu^{2+}/Aβ16($^{13}C_4$-Asp1) at pH 8.0 revealed a ^{13}C peak near the diagonal with $|a_{iso}(^{13}C_4)| < 1$ MHz, suggesting possible axial coordination of COO^{-D1} in component II.[31,32] Prior to and following these findings, Asp7 was proposed as either an equatorial[22] or an axial[35] oxygen ligand in component II. However, HYSCORE spectroscopy of Cu^{2+}/Aβ16($^{13}C^{15}N$-Asp7) at pH 8.0 provided no evidence of any ^{13}C features to support either assignment.[31] Moreover, Cu^{2+}/Aβ16($^{13}C^{15}N$-Glu3) and Cu^{2+}/Aβ16($^{13}C^{15}N$-Glu11) revealed no ^{13}C features to suggest any oxygen coordination by Glu3 or Glu11.[31]

Although component II represents a minor species in the physiologically relevant pH range, it may play a role in the production of truncated Aβ3−40/42 species[33] that are widely believed to be important in disease initiation.[38] The mechanism of generating these truncations remains uncertain, but Ala2 carbonyl coordination in component II has led to a proposed truncation mechanism involving Cu^{2+}-promoted amide hydrolysis (Figure 4).[31,33]

8. Concluding Remarks

The combination of EPR spectroscopy and isotopic labeling has provided arguably the most unambiguous determination of Cu^{2+}/Aβ coordination and future refinements of the most recent models so obtained[28,31,33,35,37] will increasingly rely on such techniques to provide credible new insights.[39] Although the possibility that $C{=}O^{D1}$ does not coordinate in both components Ia and Ib remains to be investigated (section 5), through this approach the equatorial coordination sphere of the predominating components Ia and Ib has been unraveled. One intriguing possibility is that Arg5 provides a carbonyl ligand. If so, then $^{15}N_{am}{}^{H6}$ cross peaks would be expected to appear in the HYSCORE spectra of Cu^{2+}/Aβ16(^{15}N-His6) between pH 6 and 7, analogous to the scenario for $C{=}O^{D1}$ (section 5) and $C{=}O^{A2}$ coordination (section 7), although the intense $^{15}N_{Im}{}^{H6}$ cross-peaks[28] could easily mask potentially weak $^{15}N_{am}{}^{H6}$ features. Site-specific ^{13}C-labeling of $C{=}O^{R5}$ would allow this possibility to be investigated. At higher pH, the equatorial oxygen ligand of component II has been definitively assigned, although isotopic labeling studies

have provided two alternative models of nitrogen coordination.[28,37] A re-evaluation of the multifrequency CW-EPR spectra with better signal-to-noise ratio in conjunction with more detailed pH-dependent studies of the shf structure exploiting isotopic labeling and spectral algebra will help reconcile the different results.

Isotopic labeling studies of Aβ peptides with physiologically relevant N-terminal truncations are also beginning to be carried out,[33] and additional site selective ^{13}C and ^{15}N labeling of key residues will help to further refine our understanding and relevance of their modified Cu^{2+} coordination. Of particular importance will be the translation of the above approach to the study the Cu^{2+} coordination of low molecular weight soluble Aβ oligomers. Although isolation/preparation of specific Cu^{2+}-bound oligomers for EPR studies poses a challenge, ^{15}N-labeling of soluble Aβ40 has revealed well-resolved shf structure,[28] suggesting that this approach can in principle be applied to longer peptides with adequate resolution. In lieu of such information, corresponding studies utilizing synthetic covalently cross-linked Aβ dimers[40] may provide important insight. Finally, isotopic labeling and EPR spectroscopy will be of immense value in investigating the interactions of Cu^{2+}, Aβ, and 8-hydroxyquinolines, where ternary complex formation is proposed to be responsible for some of the in vivo therapeutic effects of metal chaperones such as PBT2.[8]

BIOGRAPHICAL INFORMATION

Simon C. Drew received a B.Sc. (hons) in theoretical physics and applied mathematics in 1998 and a Ph.D. in physics in 2002 from Monash University under the supervision of John Pilbrow. Following postdoctoral research at the Centre for Magnetic Resonance, The University of Queensland, he joined the Department of Pathology, The University of Melbourne, in 2006 to study metal–protein interactions in neurodegenerative diseases. In 2010, he moved to the Max Planck Institute for Bioinorganic Chemistry. His research interests include the metallobiology of neurodegenerative disease and medical imaging.

Kevin J. Barnham received his B.Sc. in Chemistry from the University of Queensland in 1986 and his Ph.D. in 1993. His doctoral worked focused on using NMR spectroscopy to study the interactions of Pt anticancer drugs with amino acids and nucleobases under the supervision of Trevor Appleton. His postdoctoral work (1992–1995) under the supervision of Peter Sadler at Birkbeck College, The University of London expanded on this work. In 1995, he joined the Biomolecular Research Institute, The University of Melbourne, where he used NMR spectroscopy to determine the structures of proteins as potential drug targets. Since 2001, his research has focused on developing new therapeutic strategies for neurodegenerative diseases.

This work was supported in part by the National Health and Medical Research Council of Australia.

FOOTNOTES

*E-mail: drew@mpi-muelheim.mpg.de.

REFERENCES

1 Bush, A. I. The metallobiology of Alzheimer's disease. *Trends Neurosci.* **2003**, *26*, 207–214.

2 Duce, J. A.; Tsatsanis, A.; Cater, M. A.; James, S. A.; Robb, E.; Wikhe, K.; Leong, S. L.; Perez, K.; Johanssen, T.; Greenough, M. A.; Cho, H.-H.; Galatis, D.; Moir, R. D.; Masters, C. L.; McLean, C.; Tanzi, R. E.; Cappai, R.; Barnham, K. J.; Ciccotosto, G. D.; Rogers, J. T.; Bush, A. I. Iron-Export Ferroxidase Activity of β-Amyloid Precursor Protein Is Inhibited by Zinc in Alzheimer's Disease. *Cell* **2010**, *142*, 857–867.

3 Selkoe, D. J. Soluble oligomers of the amyloid β-protein impair synaptic plasticity and behavior. *Behav. Brain Res.* **2008**, *192*, 106–113.

4 Smith, D. G.; Cappai, R.; Barnham, K. J. The redox chemistry of the Alzheimer's disease amyloid beta peptide. *Biochim. Biophys. Acta* **2007**, *1768*, 1976–1990.

5 Barnham, K. J.; Bush, A. I. Metals in Alzheimer's and Parkinson's Diseases. *Curr. Opin. Chem. Biol.* **2008**, *12*, 222–228.

6 Faller, P. Copper and zinc binding to amyloid-β: coordination, dynamics, aggregation, reactivity and metal-ion transfer. *ChemBioChem* **2009**, *10*, 2691–2703.

7 Huang, X.; Cuajungco, M. P.; Atwood, C. S.; Hartshorn, M. A.; Tyndall, J. D.; Hanson, G. R.; Stokes, K. C.; Leopold, M.; Multhaup, G.; Goldstein, L. E.; Scarpa, R. C.; Saunders, A. J.; Lim, J.; Moir, R. D.; Glabe, C.; Bowden, E. F.; Masters, C. L.; Fairlie, D. P.; Tanzi, R. E.; Bush, A. I. Cu(II) potentiation of alzheimer abeta neurotoxicity. Correlation with cell-free hydrogen peroxide production and metal reduction. *J. Biol. Chem.* **1999**, *274*, 37111–37116.

8 Bush, A. I.; Tanzi, R. E. Therapeutics for Alzheimer's disease based on the metal hypothesis. *Neurotherapeutics* **2008**, *5*, 421–432.

9 Curtain, C. C.; Ali, F.; Volitakis, I.; Cherny, R. A.; Norton, R. S.; Beyreuther, K.; Barrow, C. J.; Masters, C. L.; Bush, A. I.; Barnham, K. J. Alzheimer's disease amyloid-beta binds copper and zinc to generate an allosterically ordered membrane-penetrating structure containing superoxide dismutase-like subunits. *J. Biol. Chem.* **2001**, *276*, 20466–20473.

10 Kowalik-Jankowska, T.; Ruta, M.; Wiśniewska, K.; Łankiewicz, L. Coordination abilities of the 1–16 and 1–28 fragments of β-amyloid peptide towards copper(II) ions: a combined potentiometric and spectroscopic study. *J. Inorg. Biochem.* **2003**, *95*, 270–282.

11 Karr, J. W.; Kaupp, L. J.; Szalai, V. A. Amyloid-β binds Cu^{2+} in a mononuclear metal ion binding site. *J. Am. Chem. Soc.* **2004**, *126*, 13534–13538.

12 Syme, C. D.; Nadal, R. C.; Rigby, S. E.; Viles, J. H. Copper binding to the amyloid-β peptide associated with Alzheimer's disease. *J. Biol. Chem.* **2004**, *279*, 18169–18177.

13 Karr, J. W.; Akintoye, H.; Kaupp, L. J.; Szalai, V. A. N-terminal deletions modify the Cu^{2+} binding site in amyloid-β. *Biochemistry* **2005**, *44*, 5478–5787.

14 Guilloreau, L.; Damian, L.; Coppel, Y.; Mazarguil, H.; Winterhalter, M.; Faller, P. Structural and thermodynamical properties of Cu^{II} amyloid-β16/28 complexes associated with Alzheimer's disease. *J. Biol. Inorg. Chem.* **2006**, *11*, 1024–1038.

15 Karr, J. W.; Szalai, V. A. Role of aspartate-1 in Cu(II) binding to the amyloid-β peptide of Alzheimer's disease. *J. Am. Chem. Soc.* **2007**, *129*, 3796–3797.

16 Hou, L.; Zagorski, M. G. NMR reveals anomalous copper(II) binding to the amyloid Aβ peptide of Alzheimer's disease. *J. Am. Chem. Soc.* **2006**, *128*, 9260–92615.

17 Streltsov, V. A.; Titmuss, S. J.; Epa, V. C.; Barnham, K. J.; Masters, C. L.; Varghese, J. N. The structure of the amyloid β-peptide high affinity Copper II binding site in Alzheimer's disease. *Biophys. J.* **2008**, *95*, 3447–3456.

18 Miura, T.; Suzuki, K.; Kohata, N.; Takeuchi, H. Metal binding modes of Alzheimer's amyloid β-peptide in insoluble aggregates and soluble complexes. *Biochemistry* **2000**, *39*, 7024–7031.

19 Shin, B.; Saxena, S. Direct evidence that all three histidine residues coordinate to Cu(II) in amyloid-beta1–16. *Biochemistry* **2008**, *47*, 9117–9123.

20 Peisach, J.; Blumberg, W. E. Structural implications derived from the analysis of EPR spectra of natural and artificial copper proteins. *Arch. Biochem. Biophys.* **1974**, *165*, 691–698.

21 Pilbrow, J. R. *Transition Ion Electron Paramagnetic Resonance*; Clarendon Press: Oxford, 1990.

22 Sarell, C.; Syme, C.; Rigby, S.; Viles, J. Copper(II) binding to amyloid-beta fibrils of Alzheimers disease reveals a pico-molar affinity: stoichiometry and coordination geometry is independent of Aβ Oligomeric Form. *Biochemistry* **2009**, *48*, 4388–4402.

23 Schweiger, A.; Jeschke, G. *Principles of pulse electron paramagnetic resonance*; Oxford University Press: Oxford, 2001.

24 Boas, J. F.; Pilbrow, J. R.; Smith, T. D. In *ESR of copper in biological systems*; Berliner, L. J., Reuben, J., Eds.; Biological Magnetic Resonance 1; Plenum Press: New York, 1978; pp 277−342.

25 Deligiannakis, Y.; Louloudi, M.; Hadjiliadis, N. Electron spin echo envelope modulation (ESEEM) spectroscopy as a tool to investigate the coordination environment of metal centers. *Coord. Chem. Rev.* **2000**, *204*, 1–112.

26 Millhauser, G. L. Copper and the Prion Protein: Methods, Structures, Function, and Disease. *Annu. Rev. Phys. Chem.* **2007**, *58*, 299–320.

27 Chasteen, N. D.; Snetsinger, P. A. Physical methods in bioinorganic chemistry: spectroscopy and magnetism. In *Electron paramagnetic resonance of metalloproteins*; Que, L., Ed.; University Science Books: Sausalito CA, 2000; p 213.

28 Drew, S. C.; Noble, C. J.; Masters, C. L.; Hanson, G. R.; Barnham, K. J. Pleomorphic Copper Coordination by Alzheimer's Disease Amyloid-β Peptide. *J. Am. Chem. Soc.* **2009**, *131*, 1195–1207.

29 Stoll, S.; Calle, C.; Mitrikas, G.; Schweiger, A. Peak suppression in ESEEM spectra of multinuclear spin systems. *J. Magn. Reson.* **2005**, *177*, 93–101.

30 Faller, P.; Hureau, C. Bioinorganic chemistry of copper and zinc ions coordinated to amyloid-β peptide. *Dalton Trans.* **2009**, 1080–1094.

31 Drew, S. C.; Masters, C. L.; Barnham, K. J. Alanine-2 carbonyl is an oxygen ligand in Cu^{2+} coordination of Alzheimer's disease amyloid-β peptide − relevance to N-terminally truncated forms. *J. Am. Chem. Soc.* **2009**, *131*, 8760–8761.

32 Note that an axially coordinated β-COO^- ligand and a nearby noncoordinating β-COO^- cannot be easily distinguished because both can yield a feature near the diagonal with $|a_{iso}(^{13}C)| < 1$ MHz.

33 Drew, S. C.; Masters, C. L.; Barnham, K. J. Alzheimer's Amyloid-β Peptides with Disease-Associated N-Terminal Modifications: Influence of Isomerisation, Truncation and Mutation of Residues on Cu^{2+} Coordination. *PLoS One* **2011**, *5*, e15875.

34 Iwatsubo, T; Saido, T. C.; Mann, D. M.; Lee, V. M.; Trojanowski, J. Q. Full-length amyloid-β(1−42(43)) and amino-terminally modified and truncated amyloid-β42(43) deposit in diffuse plaques. *Am. J. Pathol.* **1996**, *149*, 1823–1830.

35 Hureau, C.; Coppel, Y.; Dorlet, P.; Solari, P. L.; Sayen, S.; Guillon, E.; Sabater, L.; Faller, P. Deprotonation of the Asp1-Ala2 peptide bond induces modification of the dynamic copper(II) environment in the amyloid-β peptide near physiological pH. *Angew. Chem., Int. Ed.* **2009**, *48*, 9522–9525.

36 Van Doorslaer, S.; Cereghetti, G. M.; Glockshuber, R.; Schweiger, A. Unraveling the Cu^{2+} binding sites in the C-terminal domain of the murine prion protein: A pulse EPR and ENDOR study. *J. Phys. Chem. B* **2001**, *105*, 1631–1639.

37 Dorlet, P.; Gambarelli, S.; Faller, P.; Hureau, C. Pulse EPR spectroscopy reveals the coordination sphere of copper(II) ions in the 1−16 amyloid-β peptide: A key role of the first two N-terminus residues. *Angew. Chem., Int. Ed.* **2009**, *48*, 9273–9276.

38 Youssef, I.; Florent-Béchard, S.; Malaplate-Armand, C.; Koziel, V.; Bihain, B.; Olivier, J.-L.; Leininger-Muller, B.; Kriem, B.; Oster, T.; Pillot, T. N-truncated amyloid-β oligomers induce learning impairment and neuronal apoptosis. *Neurobiol. Aging* **2008**, *29*, 1319–1333.

39 During manuscript revision, another isotopic labeling study using ESEEM appeared, proposing that an additional $\{O, N, N_{Im}^{H13}, N_{Im}^{H14}\}$ mode contributes to component I at physiological pH (Shin, B.; Saxena, S. Substantial contribution of the two imidazole rings of the His13-His14 dyad to Cu(II) binding in amyloid-β(1−16) at physiological pH and its significance. *J. Phys. Chem. A* 2011, doi: 10.1021/jp200379m).

40 Kok, W. M.; Scanlon, D. B.; Karas, J. A.; Miles, L. A.; Tew, D. J.; Parker, M. W.; Barnham, K. J.; Hutton, C. A. Solid-phase synthesis of homodimeric peptides: preparation of covalently-linked dimers of amyloid beta peptide. *Chem. Commun.* **2009**, 6228–6230.